Structural and Functional Models for the Dinuclear Copper Active Site in Catechol Oxidases: Syntheses, X-ray Crystal Structures, Magnetic and Spectral Properties, and X-ray Absorption Spectroscopic Studies in Solid State and in Solution

Frank Zippel,[†] Friedhelm Ahlers,[†] Rüdiger Werner,[‡] Wolfgang Haase,[‡] Hans-Friedrich Nolting,[§] and Bernt Krebs*,[†]

Anorganisch-Chemisches Institut der Universität Münster, Wilhelm-Klemm-Strasse 8, 48149 Münster, Germany, Institut für Physikalische Chemie der Technischen Hochschule Darmstadt, 64287 Darmstadt, Germany, and European Molecular Biology Laboratory, Hamburg Outstation c/o DESY, Notkestrasse 85, 22603 Hamburg, Germany

Received October 20, 1995[⊗]

Two novel tridentate dinucleating ligands containing benzimidazole were prepared, 1,3-bis(2-benzimidazolyl)-2-propanol (Hbbp, **1**) and 1,5-bis(2-benzimidazolyl)-3-pentanol (Hbbpen, **2**). Their complexing properties toward copper were studied in order to obtain structural and functional models for catechol oxidases. Syntheses and crystal structures of dinuclear Cu(II) complexes derived from these ligands are reported. $[Cu_2bbp_2](ClO_4)_2 \cdot 2MeOH$, **3**, crystallizes in the triclinic space group $P\bar{1}$ with the following unit cell parameters: $a = 7.702(3)$ Å, $b = 10.973(6)$ Å, $c = 12.396(6)$ Å, $\alpha = 100.59(4)°$, $\beta = 99.02(4)°$, $\gamma = 98.90(4)°$, $V = 998.7(8)$ Å^3, and $Z = 1$. $[Cu_2bbpen_2](ClO_4)_2 \cdot 3MeOH$, **4**, crystallizes in the orthorhombic space group *Pccn*, with the following unit cell parameters: $a = 17.478(9)$ Å, $b = 18.795(8)$ Å, $c = 13.888(6)$ Å, $V = 4562.2(4)$ Å^3, and $Z = 4$. Magnetic susceptibility measurements in the temperature ranges 4.6−459 K (**3**) and 4.6−425 K (**4**) indicate an antiferromagnetic coupling between the Cu(II) centers of both complexes. In order to determine the structures of the complexes in solution, XAS spectra (EXAFS and XANES) were recorded in the solid state and in solution. The interpretation of these data, including multiple scattering calculations, together with UV−vis titrations, shows that the complexes have the same structure in the crystalline state as well as in methanolic solution. Complex **4** is able to oxidize 3,5-di-*tert*-butylcatechol (3,5-DTBC) to the quinone (catecholase activity). This reaction was also studied by XAS and UV−vis spectroscopy. These measurements reveal the reduction of Cu(II) to Cu(I) accompanied by a decrease of the coordination number.

Introduction

Copper plays an important role in biological systems, where it is mainly bound in metalloenzymes. These enzymes are involved in processes like hydroxylation, oxygen transport, electron transfer, and catalytic oxidation.

The copper containing proteins are classified into three types, Type I, Type II, and Type III. Type I, also called "blue copper", and Type II proteins both contain a mononuclear copper(II) center, whereas Type III proteins have a dinuclear active site, which is antiferromagnetically coupled and therefore EPR silent in the oxidized state.[1] The best investigated enzymes from the latter group are hemocyanin and tyrosinase.

Hemocyanin functions as an oxygen transport protein in arthropods and mollusks. Recently, X-ray diffraction studies of the deoxy form have revealed that the two noninteracting Cu(I) ions are each coordinated by three histidine N atoms. The Cu−Cu distance has been determined to 2.9−3.8 Å (the range is given from the six subunits within the hexamer) for the enzyme isolated from the spiny lobster *Panulirus interruptus*[2] and to 4.6 Å for the enzyme isolated from the horseshoe crab *Limulus polyphemus*.[3] The X-ray structure of the oxy form of the enzyme from *Limulus polyphemus* gives a Cu−Cu distance of 3.6 Å and a μ-η^2:η^2-bridging mode of the O_2^{2-} group.[4] This is consistent with EXAFS studies[5] and a dinuclear copper complex synthesized by Kitajima and co-workers.[6]

Tyrosinase catalyzes the aerial oxidation of monophenols to *o*-diphenols (cresolase activity) and the oxidation of *o*-diphenols (catechols) to *o*-quinones (catecholase activity). No X-ray crystal structure has been available until now, but spectroscopic investigations,[7] including EXAFS measurements,[8] seem to reveal that the active site is similar to that of hemocyanin.

Another Type III copper enzyme is catechol oxidase. This protein, isolated from phytogenic materials, only catalyzes the

* Author to whom correspondence should be addressed.
† Universität Münster.
‡ Technische Hochschule Darmstadt.
§ European Molecular Biology Laboratory.
⊗ Abstract published in *Advance ACS Abstracts,* May 1, 1996.

(1) (a) Lippard, S. J.; Berg, J. M. *Principles of Bioinorganic Chemistry*; University Science Books: Mill Valley, CA, 1994. (b) Kaim, W.; Schwederski, B. *Bioinorganic Chemistry*; John Wiley and Sons, Inc.: Chichester, U.K., 1994. (c) Spiro, T. G. *Copper Proteins*; John Wiley and Sons, Inc.: New York, 1981. (d) Karlin, K. D.; Tyeklár Z. *Bioinorganic Chemistry of Copper*; Chapman & Hall: New York, London, 1993.

(2) (a) Volbeda, A.; Hol, W. G. J. *J. Mol. Biol.* **1989**, *206*, 531. (b) Volbeda, A.; Hol, W. G. J. *J. Mol. Biol.* **1989**, *209*, 249.

(3) Hazes, B.; Magnus, K. A.; Bonaventura, C.; Bonaventura, J.; Dauter, Z.; Kalk, K. H.; Hol, W. G. J. *Protein Sci.* **1993**, *2*, 576.

(4) Magnus, K. A.; Hazes, B.; Ton-That, H.; Bonaventura, C.; Bonaventura, J.; Hol, W. G. J. *Proteins* **1994**, *19*, 302.

(5) (a) Brown, J. M.; Powers, L.; Kincaid, B.; Larrabee, J. A.; Spiro, T. G. *J. Am. Chem. Soc.* **1980**, *102*, 4210. (b) Co, M. S.; Scott, R. A.; Hodgson, K. O. *J. Am. Chem. Soc.* **1981**, *103*, 986. (c) Woolery, G. L.; Powers, L.; Winkler, M.; Solomon, E. I.; Spiro, T. G. *J. Am. Chem. Soc.* **1984**, *106*, 86.

(6) Kitajima, N.; Fujisawa, K.; Fujimoto, C.; Moro-oka, Y.; Hashimoto, S.; Kitagawa, T.; Toriumi, K.; Tatsumi, K.; Nakamura, A. *J. Am. Chem. Soc.* **1992**, *114*, 1277.

(7) (a) Solomon, E. I.; Penfield, K. W.; Wilcox, D. E. *Struct. Bonding (Berlin)* **1983**, *53*, 1. (b) Solomon, E. I. *Metal Clusters in Proteins*; Que, L., Jr., Ed.; American Chemical Society: Washington, DC, 1988; p 116.

(8) Woolery, G. L.; Powers, L.; Winkler, M.; Solomon, E. I.; Lerch, K.; Spiro, T. G. *Biochim. Biophys. Acta* **1984**, *788*, 155.

S0020-1669(95)01360-7 CCC: $12.00

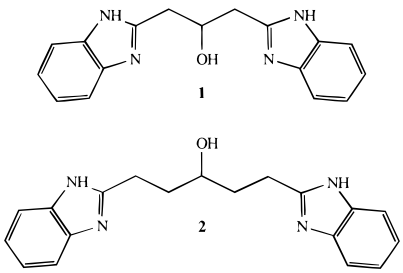

Figure 1. Ligands employed for the syntheses: 1,3-bis(2-benzimidazolyl)-2-propanol (Hbbp), **1**, and 1,5-bis(2-benzimidazolyl)-3-pentanol (Hbbpen), **2**.

oxidation of catechols to quinones without acting on tyrosine.[9] This reaction is of great importance in the medical diagnosis for the determination of the hormonal catecholamines (adrenaline, noradrenaline, and dopamine). XAS investigations on the native *met* forms from *Lycopus europaeus* and *Ipomoea batatas* have revealed that the active site consists of a dinuclear copper(II) center, where the metals are coordinated by four N/O donor ligands.[10] The Cu−Cu distance has been determined to 2.9 Å in both cases, and multiple scattering calculations have shown a high significance for one or two coordinating histidine residues.[10c] This short metal−metal distance of the native enzyme in the *met* form together with the results from EPR investigations indicates a μ-hydroxo group bridging the copper atoms. After addition of H_2O_2 the UV−vis and resonance Raman spectra are similar to the corresponding spectra of hemocyanin and tyrosinase.

The aim of this work is the synthesis and characterization of dinuclear copper complexes as structural and functional models for catechol oxidase. An often used way to get a short metal−metal distance, which has been determined for catechol oxidase by EXAFS, are dinucleating ligands with a bridging alcoholate or phenolate oxygen atom. Furthermore, for a systematic study of the multiple scattering effects of the imidazole groups (analogous to histidine in the enzyme) in the EXAFS, benzimidazole containing ligands should be used. To obtain functional models, it is necessary to have free coordination sites on the metal atom. Therefore ligands with a low number of donor atoms seem to be of great promise. Due to all the above reasons a new type of tridentate ligand has been synthesized, which is shown in Figure 1.

Furthermore, the behavior of the copper complexes formed with these ligands in solution and their reactions with 3,5-di-*tert*-butylcatechol (catecholase activity) are studied by UV−vis and XAS spectroscopy.

Experimental Section

All reagents were purchased from commercial sources and used as received. *Caution!* While none of the present perchlorate complexes has proved to be shock sensitive, care is recommended. ^{1}H NMR spectra were recorded on a Bruker WH 300 instrument; all chemical shifts are reported in parts per million (ppm) relative to an internal standard of tetramethylsilane. All elemental analyses were performed on a Hewlett-Packard Scientific Model 185. Magnetic susceptibilities of powdered samples were recorded on a Faraday-type magnetometer using a sensitive Cahn RG electrobalance in the temperature ranges 4.6−459 K (**3**) and 4.6−425 K (**4**). The magnetic field applied was ≈1.2 T. Details of the apparatus have been described elsewhere.[11] Experimental susceptibility data were corrected for the underlying diamagnetism. Corrections for diamagnetism were estimated as -540.0×10^{-6} and -581.9×10^{-6} cm^3/mol for complexes **3** and **4**, respectively.

Syntheses of Ligands and Complexes. 1,3-Bis(2-benzimidazolyl)-2-propanol (Hbbp), 1. 3-Hydroxyglutaric acid diethyl ester (20.4 g, 0.1 mol) was dissolved in 150 mL of 6 N hydrochloric acid, and 1,2-diaminobenzene (21.6 g, 0.2 mol) was added. The solution was heated to reflux and stirred at this temperature for 18 h. During this time the color turned to green. A small amount of activated carbon was added to the boiling solution, and after a few minutes the hot solution was filtered off. After cooling, a yellow precipitate was formed, which was filtered off and dissolved in 300 mL of boiling water. Concentrated aqueous ammonia was added until the solution was weakly alkaline. The obtained white crude product was filtered off, recrystallized from ethanol/water (3/2), and dried over phosphorus pentoxide, yielding 4.3 g (30%) of Hbbp. Mp: 248 °C dec. Anal. Calcd (found) for $C_{17}H_{16}N_4O$: C, 69.84 (69.78); H, 5.52 (5.59); N, 19.17 (18.94). ^{1}H NMR (dimethlyl-d_6 sulfoxide): δ 3.00 (dq, 4H), 4.60 (m, 1H), 5.60 (m, 1H), 7.00 (m, 4H), 7.45 (m, 4H) ppm.

1,5-Bis(2-benzimidazolyl)-3-pentanol (Hbbpen), 2. (a) 4-Hydroxypimelinic Acid Diethyl Ester. 4-Oxopimelinic acid diethyl ester (18.6 g, 0.081 mol) was dissolved in 75 mL of ethanol. Sodium borohydride (1.56 g, 0.046 mmol) was added while the solution was stirred at 0 °C. After 3 h of stirring at room temperature, the solution was cooled with ice and 15 mL of concentrated hydrochloric acid was added. The solution was extracted three times with 30 mL of chloroform. After evaporation 4-hydroxypimelinic acid diethyl ester was obtained as a brown-yellow oil (14.1 g, 75%).

(b) 1,5-Bis(2-benzimidazolyl)-3-pentanol. 4-Hydroxypimelinic acid diethyl ester (8.6 g, 0.038 mol) was dissolved in 60 mL of 6 N hydochloric acid, and 1,2-diaminobenzene (8.1 g, 0.075 mol) was added. The solution was heated to reflux and stirred at this temperature for 18 h. During this time the color turned to green. A small amount of activated carbon was added to the boiling solution, and after a few minutes the hot solution was filtered off. After cooling, a yellow precipitate was formed, which was filtered off and dissolved in 100 mL of boiling water. Concentrated aqueous ammonia was added until the solution was weakly alkaline. The obtained white crude product was filtered off, recrystallized from ethanol/water (3/2), and dried over phosphorus pentoxide, yielding 2.3 g (19%) of Hbbp. Mp: 262 °C dec. Anal. Calcd (found) for $C_{19}H_{20}N_4O$: C, 71.22 (71.32); H, 6.30 (6.27); N, 17.48 (17.28). ^{1}H NMR (dimethlyl-d_6 sulfoxide): δ 1.91 (m, 4H), 2.92 (m, 4H), 3.65 (m, 1H), 7.10 (m, 4H), 7.45 (m, 4H) ppm.

$[Cu_2bbp_2](ClO_4)_2\cdot 2MeOH$, 3. $Cu(ClO_4)_2\cdot 6H_2O$ (0.370 g, 1 mmol) was dissolved in 50 mL of methanol, and Hbbp (0.292 g, 1 mmol) was added while the solution was stirred. After a few hours at room temperature purple crystalline gems deposited and were collected by filtration, yielding 0.32 g (33%) of **3**. Anal. Calcd (found) for $Cu_2C_{36}H_{38}N_8O_{12}Cl_2$: C, 44.43 (43.71); H, 3.94 (3.73); N, 11.51 (11.51).

$[Cu_2bbpen_2](ClO_4)_2\cdot 3MeOH$, 4. $Cu(ClO_4)_2\cdot 6H_2O$ (0.370 g, 1 mmol) was dissolved in 25 mL of methanol, and Hbbpen (0.320 g, 1 mmol) was added while the solution was stirred. After a few days at room temperature purple needles deposited and were collected by filtration, yielding 0.29 g (27%) of **4**. Anal. Calcd (found) for $Cu_2C_{41}H_{50}N_8O_{13}Cl_2$: C, 46.41 (45.71); H, 4.75 (4.16); N, 10.56 (10.79).

X-ray Crystallography. Intensity data were collected on a Syntex $P2_1$ (**3**) and a Siemens P3 diffractometer (**4**) (Mo Kα, $\lambda = 0.710\ 73$ Å, graphite monochromator) by using the $2\theta-\omega$ scan (**3**) to a maximum 2θ value of 54° and the ω-scan (**4**) techniques to a maximum 2θ value of 42° and a variable scan rate (3−29°/min) for both complexes. As a check of crystal and electronic stability, 2 representative reflections were measured every 98 data points. No significant trend in their intensities was observed during the course of data acquisition. No extinction and absorption corrections were carried out. Further data collection parameters are summarized in Table 1.

(9) Tremolière, M.; Bieth, J. B. *Phytochemistry* **1983**, *23*, 501.
(10) (a) Rompel, A.; Büldt, K.; Krebs, B.; Fischer, H.; Meiwes, D.; Witzel, H.; Nolting, H.-F.; Hermes, C. *HASYLAB Annu. Rep.* **1993**, 691. (b) Rompel, A. Ph.D. Dissertation, University of Münster, 1993. (c) Zippel, F.; Ahlers, F.; Krebs, B.; Behning, S.; Büldt-Karentzopoulos, K.; Witzel, H.; Oversluizen, M. *Daresbury Annual Report*; Daresbury Laboratory: Daresbury, England, 1994/95; p 102. (d) Rompel, A.; Fischer, H.; Büldt-Karentzopoulos, K.; Meiwes, D.; Zippel, F.; Nolting, H.-F.; Hermes, C.; Krebs, B.; Witzel, H. *J. Inorg. Biochem.* **1995,** 59, 715.
(11) (a) Merz, L.; Haase, W. *J. Chem. Soc., Dalton Trans.* **1980**, 875. (b) Walz, L.; Paulus, H.; Haase, W. *J. Chem. Soc., Dalton Trans.* **1985**, 913.

Table 1. Crystallographic Data for the Complexes

	3	**4**
formula	$Cu_2C_{36}H_{38}N_8O_{12}Cl_2$	$Cu_2C_{41}H_{50}N_8O_{13}Cl_2$
M_r	972.72	1061.87
cryst dimens, mm	0.20 × 0.24 × 0.12	0.30 × 0.35 × 0.80
space group	$P\bar{1}$, triclinic	*Pccn*, orthorhombic
a, Å	7.702(3)	17.478(9)
b, Å	10.973(6)	18.795(8)
c, Å	12.396(6)	13.888(6)
α, deg	100.59(4)	90.0
β, deg	99.02(4)	90.0
γ, deg	98.90(4)	90.0
V, Å^3	998.7(8)	4562.2(4)
Z	1	4
T, K	150 K	150 K
ρ_{calcd}, g cm^{-3}	1.617	1.545
μ, mm^{-1}	1.27	1.12
transm factors: max, min	0.74, 0.86	0.41, 0.71
index ranges	$-9 \le h \le 9$ $-14 \le k \le 13$ $0 \le l \le 15$	$0 \le h \le 22$ $0 \le k \le 24$ $0 \le l \le 17$
tot. no. of unique data	4372	2445
no. of data, $I > 2\sigma(I)$	3514	996
no. of params refined	273	300
R1 [$I > 2\sigma(I)$], wR2 [all data][a]	0.0347, 0.0876	0.0650, 0.1849
weighting scheme, w^{-1} [b]	$\sigma^2(F_o^2) + (0.0442P)^2 + (0.3107P)$	$\sigma^2(F_o^2) + (0.1030P)^2$
goodness of fit	1.053	0.811

[a] $R1 = \sum||F_o| - |F_c||/\sum|F_o|$, $wR2 = [\sum w(F_o^2 - F_c^2)^2/\sum w(F_o^2)^2]^{1/2}$. [b] $P = (F_o^2 + 2F_c^2)/3$.

The structures were solved by direct (**3**) or Patterson and Fourier methods (**4**) (program XS[12]). A series of full-matrix least-squares refinement cycles on F^2 (program SHELXL-93[13]) followed by Fourier syntheses gave all remaining non-hydrogen atoms. The hydrogen atoms in both structures were placed at calculated positions and constrained to "ride" on the atom to which they are attached. The isotropic thermal parameters for the methyl and hydroxyl protons were refined with 1.5 times and for all other hydrogen atoms with 1.2 times the U_{eq} value of the corresponding atom. All other atoms of the complex molecules in **3** and **4** were refined anisotropically, with the exception of C(1) in **4**, which was refined isotropically. With the exception of one disordered solvent molecule in **4** (K(O(7)) = K(O(7a)) = 0.5) the occupancy factors for all other atoms in **3** and **4** are $K = 1$. Final atomic coordinates and isotropic thermal parameters of compounds **3** and **4** are listed in Tables 2 and 3, respectively.

X-ray Absorption Measurements. Models in the Solid State. Microcrystalline samples of complexes **3** and **4** were prepared according to ref 14. The X-ray absorption spectra at the Cu K edge were recorded at the European Molecular Biology Laboratory (c/o DESY, Hamburg) using the synchrotron radiation from the storage ring DORIS III.[15] Data collection was performed at ca. 4.5 GeV and a maximum current of 120 mA. A Si(111) double crystal monochromator was used with a typical energy resolution of 1.5 eV.[15a] Harmonic rejection was accomplished by detuning the first monochromator crystal by 70%. The spectra were recorded at 20 K in transmission mode by using a modified Oxford Instruments cryostat and ionization chambers (Ar/CO_2) over the energy range from 8580 to 9980 eV. To check for reproducibility and to improve counting statistics, at least two individual spectra were recorded for both samples and averaged.

Table 2. Atomic Coordinates and Isotropic Thermal Parameters (Å^2) for Non-Hydrogen Atoms in **3**

atom	*x*	*y*	*z*	U_{eq}
Cu(1)	0.33923(4)	0.46553(3)	0.40488(2)	0.01360(9)
N(1)	0.1554(3)	0.5617(2)	0.3652(2)	0.0153(4)
N(2)	0.0441(3)	0.7328(2)	0.3485(2)	0.0171(4)
N(3)	0.2621(3)	0.3150(2)	0.2844(2)	0.0141(4)
N(4)	0.2637(3)	0.1191(2)	0.1996(2)	0.0176(4)
O(1)	0.4851(2)	0.6076(2)	0.5138(2)	0.0162(4)
O(2)	0.2959(4)	1.0416(3)	0.6390(3)	0.0631(8)
O(3)	0.0115(3)	1.0288(2)	0.6873(2)	0.0313(5)
O(4)	0.0885(3)	0.8498(2)	0.5869(2)	0.0372(5)
O(5)	0.2257(4)	0.9280(2)	0.7726(2)	0.0523(7)
O(6)	0.3768(3)	−0.1160(2)	0.1784(2)	0.0456(6)
Cl(1)	0.15525(9)	0.96176(6)	0.67042(5)	0.0218(2)
C(1)	0.4534(3)	0.7326(2)	0.5392(2)	0.0140(5)
C(2)	0.3692(3)	0.7694(2)	0.4324(2)	0.0168(5)
C(3)	0.1909(3)	0.6877(2)	0.3821(2)	0.0152(5)
C(4)	−0.0274(3)	0.5238(2)	0.3178(2)	0.0161(5)
C(5)	−0.1353(3)	0.4046(3)	0.2812(2)	0.0211(5)
C(6)	−0.3121(4)	0.3987(3)	0.2314(2)	0.0237(6)
C(7)	−0.3792(4)	0.5086(3)	0.2207(2)	0.0260(6)
C(8)	−0.2746(3)	0.6273(3)	0.2590(2)	0.0219(5)
C(9)	−0.0972(3)	0.6321(2)	0.3073(2)	0.0157(5)
C(10)	0.6286(3)	0.8250(2)	0.5928(2)	0.0170(5)
C(11)	0.2962(3)	0.2023(2)	0.2973(2)	0.0151(5)
C(12)	0.2031(3)	0.3026(2)	0.1693(2)	0.0154(5)
C(13)	0.1553(3)	0.3902(2)	0.1076(2)	0.0180(5)
C(14)	0.1080(4)	0.3491(3)	−0.0076(2)	0.0235(6)
C(15)	0.1062(4)	0.2242(3)	−0.0597(2)	0.0264(6)
C(16)	0.1535(4)	0.1364(3)	−0.0001(2)	0.0222(6)
C(17)	0.2041(3)	0.1785(2)	0.1160(2)	0.0170(5)
C(18)	0.3832(5)	−0.1811(4)	0.0692(4)	0.0666(13)

Table 3. Atomic Coordinates and Isotropic Thermal Parameters (Å^2) for Non-Hydrogen Atoms in **4**

atom	*x*	*y*	*z*	U_{eq}
Cu(1)	0.17751(7)	0.20641(8)	0.12778(10)	0.0498(5)
N(1)	0.0693(5)	0.2297(5)	0.1559(7)	0.056(3)
N(2)	−0.0418(7)	0.2798(7)	0.1527(10)	0.096(5)
N(3)	0.1543(5)	0.1127(5)	0.0763(7)	0.053(3)
N(4)	0.1601(5)	−0.0030(5)	0.0403(7)	0.054(3)
O(1)	0.2135(3)	0.3034(4)	0.1280(5)	0.050(2)
O(2)	0.2136(11)	0.5221(15)	0.8916(11)	0.443(22)
O(3)	0.1238(7)	0.5684(9)	0.8025(10)	0.215(9)
O(4)	0.1553(7)	0.6248(8)	0.9446(12)	0.189(7)
O(5)	0.1125(20)	0.5292(14)	0.9422(25)	0.415(22)
O(6)	0.2085(6)	−0.1452(6)	0.0546(10)	0.124(4)
O(7)	0.1878(13)	0.1969(17)	0.3225(18)	0.204(14)
Cl(1)	0.1566(4)	0.5630(5)	0.8867(5)	0.157(3)
C(1)	0.1709(10)	0.3590(9)	0.1784(13)	0.120(6)
C(2)	0.1222(12)	0.3942(10)	0.1078(12)	0.183(11)
C(3)	0.0673(12)	0.3406(8)	0.0451(12)	0.145(9)
C(4)	0.0305(7)	0.2845(8)	0.1175(10)	0.071(4)
C(5)	0.0211(7)	0.1879(8)	0.2167(10)	0.066(4)
C(6)	0.0334(9)	0.1278(9)	0.2727(11)	0.086(5)
C(7)	−0.0257(13)	0.1028(10)	0.3253(12)	0.116(7)
C(8)	−0.0966(13)	0.1366(14)	0.3198(17)	0.143(11)
C(9)	−0.1132(11)	0.1944(13)	0.2673(16)	0.139(9)
C(10)	−0.0495(8)	0.2233(11)	0.2148(13)	0.093(5)
C(11)	0.2755(10)	0.0849(9)	0.2281(15)	0.147(8)
C(12)	0.2447(8)	0.0312(7)	0.1673(10)	0.081(5)
C(13)	0.1859(6)	0.0510(8)	0.0970(8)	0.049(3)
C(14)	0.1048(6)	0.0996(8)	−0.0029(9)	0.048(3)
C(15)	0.0586(6)	0.1446(7)	−0.0520(9)	0.058(4)
C(16)	0.0159(6)	0.1160(8)	−0.1256(11)	0.065(4)
C(17)	0.0207(7)	0.0422(9)	−0.1469(9)	0.067(4)
C(18)	0.0671(7)	−0.0038(7)	−0.0988(9)	0.063(4)
C(19)	0.1086(6)	0.0280(8)	−0.0244(9)	0.053(3)
C(20)	0.3341(9)	0.6938(9)	1.0125(16)	0.159(9)
C(21)	0.2500	0.2500	0.3819(20)	0.260(23)

The energy calibration was done by rescaling the energy axis of the spectrometer to absolute values with a number of Bragg reflections obtained by an oriented Si crystal.[15a]

(12) Sheldrick, G. M. *SHELXTL PLUS*, Siemens Analytical X-ray Instruments, University of Göttingen: Göttingen, Germany, 1990.
(13) Sheldrick, G. M. *SHELXL-93*, Program for Crystal Structure Determination, University of Göttingen: Göttingen, Germany, 1993.
(14) Nolting, H.-F.; Tremel, W.; Eggers, P.; Henkel, G.; Krebs, B. *Nucl. Instrum. Methods Phys. Res. A* **1987**, *259*, 576.
(15) (a) Pettifer, R. F.; Hermes, C. *J. Appl. Crystallogr.* **1985**, *18*, 404. (b) Hermes, C.; Gilberg, E.; Koch, M. H. J. *J. Nucl. Instrum. Methods* **1984**, *222*, 207. (c) Pettifer, R. F.; Hermes, C. *J. Phys. (Paris)* **1986**, *C8*, 127.

Models in Solution. Three concentrated methanolic solutions were prepared. Because the alcohol function of the ligands deprotonates during the formation of the complexes, the reactions depend on the pH value. Therefore it is necessary to work with buffered solutions. As buffer, 2,4,6-collidine/$HClO_4$ (2:1) was used in a 50-fold surplus. This system is very suitable, because collidine itself is a weak ligand for Cu(II). Due to its steric inhibition it does not coordinate as long as other, better ligands are present, which was examined by UV−vis spectroscopy by comparing spectra with and without this and other buffers. The supposition that collidine is a weak ligand is also in agreement with the results of this work. Other advantages of this buffer system are the high solubility in methanol and the neutral buffer range. The following samples were prepared:

1. $Cu(ClO_4)_2 \cdot 6H_2O$ (14.8 mg, 0.04 mmol) and Hbbp (11.7 mg, 0.04 mmol) were dissolved in 10 mL buffered methanol (**3** in solution).

2. $Cu(ClO_4)_2 \cdot 6H_2O$ (37.0 mg, 0.1 mmol) and Hbbpen (32.0 mg, 0.1 mmol) were dissolved in 10 mL buffered methanol (**4** in solution).

3. $Cu(ClO_4)_2 \cdot 6H_2O$ (14.8 mg, 0.04 mmol) and Hbbpen (11.7 mg, 0.04 mmol) were dissolved in 10 mL buffered methanol, and 3,5-di-*tert*-butylcatechol (88.9 mg, 0.4 mmol) was added (**4** in solution after addition of 3,5-DTBC).

The samples were enclosed in appropriate cells with kapton foil windows.

These samples were measured on beam line 8.1 at the SRS, Daresbury Laboratory, with an electron beam energy of 2.0 GeV and a maximum current of 325 mA. A Si(220) double crystal monochromator was used with a detuning of 70%. The energy ranged from 8870 to 9730 eV. The spectra were recorded in fluorescence mode using a 13-element Ge detector at room temperature, because it was not possible to freeze the samples without getting Bragg reflections in the spectra, with the exception of sample 2, which could be measured at 80 K in frozen solution without Bragg reflections. Approximately five individual spectra were recorded and averaged for each sample.

The energy calibration was achieved by setting the first inflection point of a copper foil spectrum to 8980.3 eV, the resolution was estimated to about 1 eV.

Analysis of the XAS Data. The background subtraction, the normalization of the spectra, the determination of the edge position, and the extraction of the fine structure have been performed as described earlier.[16] An E_0 value of 8982.0 eV has been used for the data reduction. The $\chi(k)$ values were multiplied by k^3 and transformed by Fourier procedures.

Prior to curve-fitting analyses, the individual peaks in these functions were back-transformed into single-shell EXAFS spectra according to the Fourier filtering approach. In order to include the multiple scattering effects of the imidazole ligands, we also performed wide-shell filtered spectra.[17] The width of the windows used for the back-transformations from R to k space are stated in the corresponding tables.

The final data analysis was carried out by least-squares curve fitting using a full curved wave approach from the program EXCURV92.[18] For the single-shell filtered data the number of scatterers (cn), the absorber−scatterer distance (R), the Debye−Waller factors (σ^2), and the value E_0 were refined.

The fitting of the wide-shell filtered data was done by constrained refinement of the imidazole groups, including their multiple scattering contributions as described in ref 19. The imidazole rings are treated as a geometrically rigid unit. The values for the bond lengths and angles were taken from their crystallographic data and not refined. For a further reduction of the parameter the assumption is made that chemically similar atoms in a similar distance have the same Debye−Waller factor.[19] Therefore only the one distance R_a, the angle ϕ, which describes the rotation of the ring about an axis through the coordinated N and perpendicular to the ring plane, and three Debye−Waller factors ($\sigma^2(N_a)$, $\sigma^2(C_a) = \sigma^2(C_b)$, $\sigma^2(N_b) = \sigma^2(C_c)$) are refined for the imidazole units (see Figure 2). The angle between the plane of the ring and an axis collinear with the Cu−N bond is not refined, because it is found that the EXAFS is relatively insensitive to a variation of this angle.[20] Additional shells are fitted in the same way as described under single-shell fits. The value E_0 is refined for all shells together.

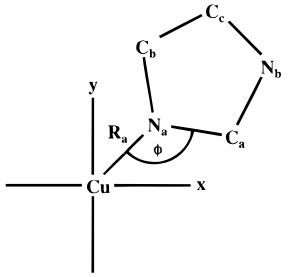

Figure 2. Atom labeling and parameter definition of the imidazole group (lying in the $x-y$ plane).

We used a value of 0.7 for the amplitude reduction factor and −1 eV for the constant imaginary potential, which describes the lifetime of the photoelectrons.

The unfiltered data were also fitted. The quality of these fits was generally worse because of the increased noise level, but the results were similar and consistent with those of the wide-shell filtered data.

The quality of the fit is represented by the R-factor, which is given as

$$R = \sum_i \frac{k_i^3}{\sum_j k_j^3 |\chi_j^{exp}(k_j)|} |\chi^{exp}(k_i) - \chi^{th}(k_i)| \times 100\%$$

where $\chi^{exp}(k)$ and $\chi^{th}(k)$ are the experimental and theoretical EXAFS.[18]

The maximum number of parameters allowed to vary simultaneously in the curve fitting analyses were estimated by $N_{free} = 2\Delta R_{FF}\Delta k_{fit}/\pi$, where ΔR_{FF} is the width of the filter window and Δk_{fit} is the length of the data set in k space.

UV−Vis Spectroscopy. Electronic spectra were recorded on a Shimadzu UV-3100 spectrophotometer. Ligand binding studies were performed by adding methanolic solutions of copper perchlorate to solutions of the ligands at room temperature. The reaction of the complexes with 3,5-di-*tert*-butylcatechol was studied by adding different concentrated catechol solutions to the complexes and recording the spectra in different time intervals also at room temperature. In all cases 2,4,6-collidine/$HClO_4$ (2:1) was used as buffer in a 50-fold surplus due to the above stated reasons.

Results and Discussion

I. Investigations in Solid State. Description of the X-ray Structure of $[Cu_2bbp_2](ClO_4)_2 \cdot 2MeOH$, 3. Compound **3** crystallizes in the triclinic space group $P\bar{1}$. The structure of the cation is shown in Figure 3, and selected bond lengths and angles are given in Tables 4 and 5, respectively.

The cation contains a dinuclear copper center in which the metal atoms are coordinated by two ligand molecules. The inversion center is located between the two copper atoms (Cu−Cu: 3.033 Å) so that they are structurally equivalent. Both metal atoms are coordinated in a distorted square planar environment by two benzimidazole nitrogen atoms and two bridging alkoxo oxygen atoms. The Cu−O and Cu−N bond lengths are comparable to those of other copper complexes. According to the symmetry, the two copper and the two oxygen atoms form an exact plane. Because of the steric force of the chelating ligands, one of the two coordinating nitrogen atoms

(16) Priggemeyer, S.; Eggers-Borkenstein, P.; Ahlers, F.; Henkel, G.; Körner, M.; Witzel, H.; Nolting, H.-F.; Hermes, C.; Krebs, B. *Inorg. Chem.* **1995**, *34*, 1445.
(17) DeWitt, J. G.; Bentsen, J. G.; Rosenzweig, A. C.; Hedman, B.; Green, J.; Pilkington, S.; Papaefthymiou, G. C.; Dalton, H.; Hodgson, K. O.; Lippard, S. J. *J. Am. Chem. Soc.* **1991**, *113*, 9219.
(18) Binsted, N.; Campbell, J. W.; Gurman, S. J.; Stephenson, P. C. SERC Daresbury Laboratory EXCURV92 program, 1992.
(19) Binsted, N.; Strange, R. W.; Hasnain, S. S. *Biochemistry* **1992**, *31*, 12117.
(20) Blackburn, N. J.; Hasnain, S. S.; Pettingill, T. M.; Strange, R. W. *J. Biol. Chem.* **1991**, *266*, 23120.

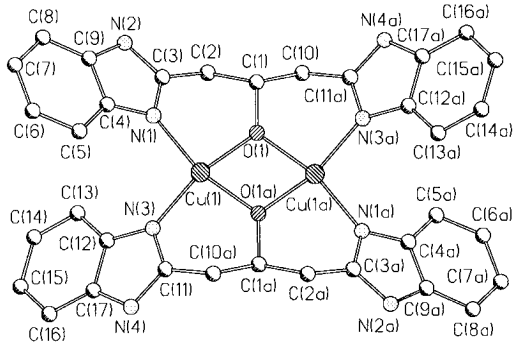

Figure 3. Molecular structure and atomic numbering scheme for the cation of $[Cu_2bbp_2](ClO_4)_2 \cdot 2MeOH$, **3**. Hydrogen atoms are omitted for clarity.

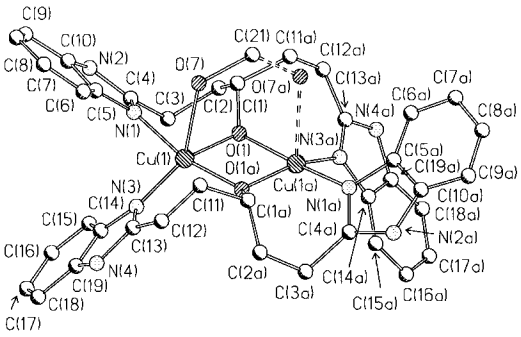

Figure 4. Molecular structure and atomic numbering scheme for the cation of $[Cu_2bbpen_2](ClO_4)_2 \cdot 3MeOH$, **4**. Hydrogen atoms are omitted for clarity.

Table 4. Selected Interatomic Distances (Å) for **3** and **4**

3		**4**	
Cu(1)···Cu(1a)	3.033(2)	Cu(1)···Cu(1a)	3.017(3)
Cu(1)−O(1)	1.930(2)	Cu(1)−O(1)	1.927(7)
Cu(1)−O(1a)	1.923(2)	Cu(1)−O(1a)	1.913(6)
Cu(1)−N(1)	1.948(2)	Cu(1)−N(1)	1.981(9)
Cu(1)−N(3)	1.955(2)	Cu(1)−N(3)	1.945(10)
		Cu(1)−O(7)	2.690(25)

Table 5. Selected Interatomic Angles (deg) for **3** and **4**

3		**4**	
N(1)−Cu(1)−N(3)	100.1(1)	N(1)−Cu(1)−N(3)	94.3(4)
N(3)−Cu(1)−O(1a)	93.3(1)	N(3)−Cu(1)−O(1a)	96.9(3)
O(1a)−Cu(1)−O(1)	76.2(1)	O(1a)−Cu(1)−O(1)	76.4(3)
O(1)−Cu(1)−N(1)	92.8(1)	O(1)−Cu(1)−N(1)	95.9(3)
Cu(1)−O(1)−Cu(1a)	103.9(1)	Cu(1)−O(1)−Cu(1a)	103.6(3)

lies above this plane, the other one below it. Their distances from the plane are 0.408 and 0.469 Å.

The six-membered chelate rings formed by the ligands have a twisted conformation. Both benzimidazole rings of each ligand molecule are found on the same side of the space which is divided by the mentioned plane.

Description of the X-ray Structure of $[Cu_2bbpen_2](ClO_4)_2 \cdot 3MeOH$, 4. Compound **4** crystallizes unambiguously in the orthorhombic space group *Pccn*. The structure of the cation is shown in Figure 4, and selected bond lengths and angles are given in Tables 4 and 5, respectively.

The structure is similar to that of **3**. The cation again contains a dinuclear copper center, where the metal atoms are coordinated by two ligand molecules. The 2-fold crystallographic axis lies between the two copper atoms (Cu−Cu: 3.017 Å). Both metal atoms are coordinated by two benzimidazole nitrogen atoms and two bridging alkoxo oxygen atoms. The Cu−O and Cu−N bond lengths lie again in the range of other copper complexes. In addition, one of the two copper atoms is coordinated by the oxygen atom of the disordered methanol, the carbon atom of which lies on the 2-fold axis between the metal atoms. Thus, one copper atom has a distorted square planar and the other a distorted square pyramidal environment. The two copper atoms and the two alkoxo oxygen atoms form a nearly exact plane. Equal to **3** again, one of the two coordinating nitrogen atoms lies above this plane, the other one below it. Their distances from the plane are 0.389 and 0.717 Å.

In contrast to **3**, the ligands form seven-membered chelate rings and, due to the 2-fold axis, both benzimidazole rings of each ligand molecule are found on the opposite side of the space which is divided by the mentioned plane.

The disordered methanol led to some problems during the refinement procedure. It was not possible to refine C(1) anisotropically. For the other carbon atoms of the chelating rings unusual large thermal ellipsoids were obtained, which are not caused by thermal vibrations, but by the static disorder. The attempt to split their positions led to unreasonable values for the distances and angles. The static disorder manifests itself also in the bad signal to noise ratio of the outer reflections. Therefore we had to exclude all reflections with $\theta > 21.1°$. The limited number of data caused relatively high estimated standard deviations (esd's), but the average distance values of similar bonds are in good agreement with known values.

Magnetic Properties. Solid state magnetic susceptibility measurements on polycrystalline samples of **3** and **4** were made by using the Faraday method in the temperature range between 4.6 and 459 K (**3**) and between 4.6 and 425 K (**4**). For the fitting procedure of **3** only values above 65 K have been taken into consideration, because of not absolutely reproducible behavior at lower temperatures caused by an unexpected effect at 50 K which has to be explained by further investigations. For both complexes the obtained values and curves of the susceptibility and μ_{eff} versus temperature are typical for strong antiferromagnetic coupling between the two $S = {}^1/_2$ copper(II) ions in dinuclear complexes. The room temperature values for μ_{eff} are 0.44 μ_B (**3,** 300.4 K) and 0.85 μ_B (**4,** 299.8 K), which is less than the value of 1.73 μ_B for a free copper(II) ion. The magnetic moments of both complexes decrease at 4.6 K to ca. 0.15 μ_B (**3**) and 0.21 μ_B (**4**). The values could be fitted on the basis of an isotropic Heisenberg model, $H' = -2JS_1S_2$ ($S_1 = S_2 = {}^1/_2$).[21] The temperature-independent paramagnetism has been determined to 30×10^{-6} cm^3/mol (**3**) or was fixed to 60×10^{-6} cm^3/mol (**4**) for each copper atom, respectively. A correction for a small amount of paramagnetic impurity (χ_p) was taken into account. The best parameters obtained were as follows: for **3**, $g = 2.20(3)$, $2J = -1020(40)$ cm^{-1}, and $\chi_p = 0.4(2)$%, and for **4**, $g = 2.08(4)$, $2J = -630(30)$ cm^{-1}, and $\chi_p = 3.3(3)$%. Merz and Haase have shown that the exchange parameter $2J$ is linearly correlated with the Cu−O−Cu angle of alkoxo bridged copper(II) dimers.[11a] According to this relationship a value of $2J < -600$ cm^{-1} would be expected for complex **4**, which is in good agreement with the stated results. The exchange coupling of **3** is significantly stronger as the expected value derived from this correlation. Walz et al.[11b] have shown that the coordination geometry is also an important factor. They have found that the exchange parameter $2J$ depends on the size of the distortion from an ideal square planar coordination. The coordination geometry of **3** is very similar to that described by Walz et al., who have also found values for $2J$ in the range of -1000 to -1100 cm^{-1}. In both cases the the copper ion and the bridging oxygen are integrated in a six-membered ring compared to the five- or seven-membered rings in ref 11 and **4**.

(21) O'Connor, C. J. *Prog. Inorg. Chem.* **1982**, *29*, 203.

Table 6. Results of the First Shell Fits[a] and the Second Shell Fits[a] (Metal−Metal Contribution) by Curve-Fitting Analysis of the Complexes in Solid State and Comparison with the Crystallographic Data

	EXAFS							X-ray cryst	
complex	window width,[b] Å	N_{free}[c]	cn[d] and scatterer	R, Å	σ^2, Å^2	E_0	R-factor,[c] %	cn[d] and scatterer	R, Å
				First Shell					
3	1.1−2.0	8	3.6 O	1.924	0.002	11.8	13.3	2 N and 2 O	1.939[e]
			or 4.5 N	1.940	0.002	13.9	12.8		
4	1.0−2.0	9	3.8 O	1.924	0.003	11.6	13.7	2 N and 2 O	1.942[e]
			or 4.5 N	1.941	0.003	13.0	14.8		
				Second Shell					
3	2.5−3.1	5	0.7 Cu	3.028	0.001	13.1	17.1	1 Cu	3.033
4	2.3−3.2	8	1.0 Cu	3.000	0.002	5.3	23.9	1 Cu	3.017

[a] The Fourier transform range is $k = 1.8-16.1$ Å^{-1}. [b] The window width for Fourier filtering is given in reduced angstroms. [c] As defined in the Experimental Section. The number of refined parameters is 4 for all fits and therefore less than the maximum number of free parameters. [d] cn = coordination number. [e] The values are the averaged distances of the crystallographic data of the four atoms of the first shell.

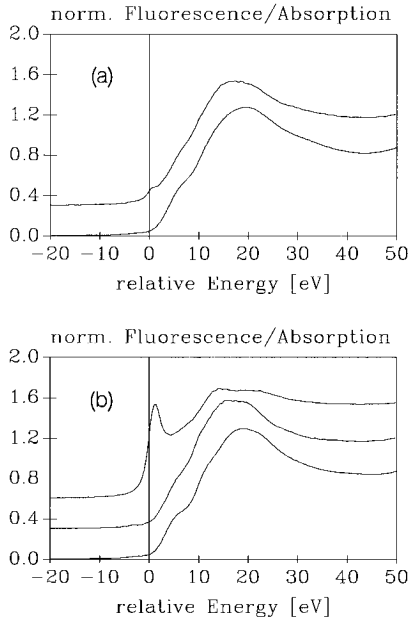

Figure 5. XANES spectra of **3**, (a) in the solid state (bottom) and in solution (top), and XANES spectra of **4**, (b) in the solid state (bottom), in solution (middle), and after addition of 3,5-di-*tert*-butylcatechol (top). Energy zero at 8982.0 eV.

X-ray Absorption Spectroscopy. Figure 5 shows the XANES spectra of **3** and **4** in the solid state. The edge positions (inflection points) are 8992.5 and 8992.0 eV, respectively. Both spectra exhibit a very low pre-edge peak at about 8979 eV, which has been proposed and later confirmed as a 1s → 3d transition[22,23] and a shoulder at about 8989 eV, which has been assigned as a 1s → 4p transition.[24,25] The positions and the intensities of these features are typical for Cu(II) with a four-coordination by N/O donors.[24a,10b]

Fourier-filtered EXAFS data (the window widths are given in Table 6) were used for initial curve-fitting analysis of the first shell and the second shell (metal−metal contribution). A comparison between the fit results and the crystallographic values is shown in Table 6. The first shell of the complexes consists of two nitrogen and two oxygen atoms, apart from the disordered methanol in **4**, which was not included into the EXAFS fits, because of the low significance of a half-coordinating molecule relating to each copper atom.

EXAFS fits with such a split first shell did not yield satisfying results, because of the high correlation between the parameters of these subshells. Since the amplitude and phase functions of the two adjacent elements in the periodic table are very similar, it is not necessary to fit with two subshells if the absorber−scatterer distances do not vary much. Therefore we performed two different fits, one with oxygen and one with nitrogen amplitude and phase functions. The fits with the nitrogen functions always result in a slightly higher coordination number and a slightly higher distance than the fits with the oxygen functions, but this is in the range of the estimated errors, which are about ±1 for coordination numbers and ±0.03 Å for distances.[17] The comparison of the structural parameters derived from EXAFS and X-ray crystallography indicates the high accuracy of the EXAFS technique, especially for the determination of distances.

Normally, the determination of metal−metal distances is more complicated, because of low-Z scatterers (here C) at a similar radial distance, especially around 3.0 Å.[26] Therefore the problem of most EXAFS determinations of metal−metal distances is that there are often a few possibilities to fit a metal−metal contribution and/or low-Z scatterer contribution. Often it is not possible to decide which of the different fits is the right one. A lot of different techniques have been developed and tested, but none of them leads to an absolutely reliable result.[16,26] In our case this problem is easier to solve, because from X-ray crystallography we know which peak in the Fourier transform of the k^3-weighted fine structure contains the metal−metal contribution. Then the determination of the metal−metal distance is very reliable and accurate, even with Fourier-filtered data. The relatively high R-factors of the second shell fits compared to those of the first shell fits are due to the contributions of the carbon atoms of the benzimidazole ligands, which have a similar absorber distance.

In order to include the multiple scattering effects of the benzimidazole groups of the ligands, we also performed multiple scattering calculations using constraint refinement of the imidazole rings. The two structural known compounds are models to test if it is possible to get an indication of the number of coordinating imidazole groups. It shall also be tested if the significance of the determination of the metal−metal distance can be improved by multiple scattering calculations.

For a better comparison with the data of the complexes in solution, which are of lower quality, we used a similar fitting

(22) Shulman, R. G.; Yafet, T.; Eisenberger, P.; Blumberg, W. E. *Proc. Natl. Acad. Sci. U.S.A.* **1976**, *73*, 1384.
(23) Hahn, J. E.; Scott, R. A.; Hodgson, K. O.; Doniach, S.; Desjardins, S. E.; Solomon, E. I. *Chem. Phys. Lett.* **1982**, *88*, 595.
(24) (a) Kau, L.-S.; Spira-Solomon, D. J.; Penner-Hahn, J. E.; Hodgson, K. O.; Solomon, E. I. *J. Am. Chem. Soc.* **1987**, *109*, 6433. (b) Shadle, S. E.; Penner-Hahn, J. E.; Schugar, H. J.; Hedman, B.; Hodgson, K. O.; Solomon, E. I. *J. Am. Chem. Soc.* **1993**, *115*, 767.
(25) Pickering, I. J.; George, G. N. *Inorg. Chem.* **1995**, *34*, 3142.
(26) Scott, R. A.; Eidsness, M. K. *Comments Inorg. Chem.* **1988**, *7*, 235.

Table 7. Results of the Wide-Shell Fits[a] with the Lowest *R*-Factors Using Multiple Scattering Calculations and Constrained Refinement of the Imidazole Groups

complex	window width,[b] Å	N_{free}[c]	cn[d] and scatterer	*R*, Å	σ^2, Å^2	E_0	ϕ, deg	*R*-factor,[c] %
3	1.0−4.0	17	2 O	*1.956*	*−0.005*	*15.9*	*123.4*	16.5
			2 N (imi)	*1.844*	*−0.004*			
			2 C (imi)	2.812	*0.001*[e]			
			2 C (imi)	2.953	0.001[e]			
			2 N (imi)	3.980	*0.010*[f]			
			2 C (imi)	4.131	0.010[f]			
			1 Cu	*3.016*	*0.002*			
4	1.0−4.0	17	2 O	*1.978*	*−0.002*	*15.3*	*122.7*	14.2
			2 N (imi)	*1.854*	*0.001*			
			2 C (imi)	2.811	*0.001*[e]			
			2 C (imi)	2.970	0.001[e]			
			2 N (imi)	3.984	*0.014*[f]			
			2 C (imi)	4.143	0.014[f]			
			1 Cu	*2.965*	*0.001*			

[a] The Fourier transform range is $k = 2.5-11.5$ Å^{-1}. [b] The window width for Fourier filtering is given in reduced angstroms. [c] As defined in the Experimental Section. The number of refined parameters is 10 and therefore less than the maximum number of free parameters. [d] cn = coordination number, not refined. [e] Refined together. [f] Refined together, see Experimental Section. All refined parameters in italics.

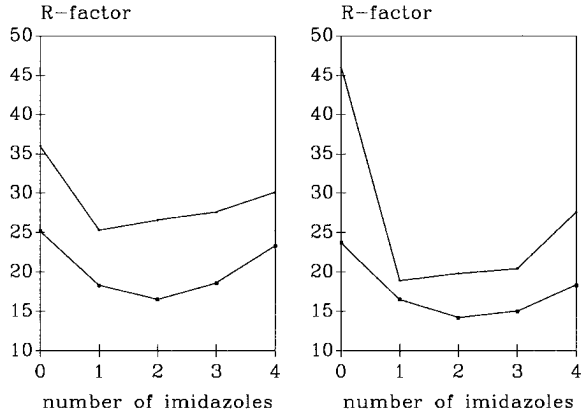

Figure 6. Dependence of the *R*-factor from the number of imidazoles of **3** (left) and **4** (right) in the solid state, (no. of oxygen atoms in the first shell) = 4 − (no. of imidazoles): without the Cu−Cu contribution (top); with the Cu−Cu contribution (bottom).

range ($k = 2.5-11.5$ Å^{-1}). The results of the fits over the whole data range ($k = 1.8-16.1$ Å^{-1}) are very similar to those, and the trends (see below) are all the same. Thus the effect of the fitting range is only small.

The fitting procedure is described in the Experimental Section. Because the first shell of the models consists of oxygen and imidazole nitrogen atoms, we performed fits which differ from each other by the number of oxygen and nitrogen atoms, whereby their sum was always 4, which is the coordination number. All fits were performed with and without the additional scatterer contribution of the second copper atom. The dependence of the *R*-factor of the fits on these variations is shown in Figure 6 for both complexes.

The results are very similar for both compounds. The *R*-factors of the fits without imidazoles and without the second metal are very high, because in these cases there is no possibility to fit any contribution of the atoms in higher shells.

In all cases the fits with the Cu−Cu scattering contribution are significantly better than the fits without it. The *R*-factor is not the only indication for the presence of a second metal. The calculations without Cu−Cu contributions are not able to fit the peak at ca. 3 Å in the Fourier transform of the k^3-weighted fine structure adequately and often result in negative Debye−Waller factors for the α-carbon atoms of the imidazole rings in this shell.

The determination of the number of coordinating imidazoles does not lead to such a definite result. Indeed, the best fits are

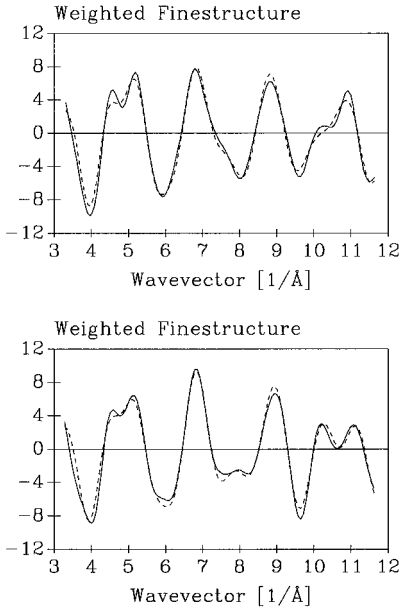

Figure 7. Comparison of the k^3-weighted fine structures of the filtered data (solid lines) and the fits (dashed lines) of **3** (top) and **4** (bottom) in the solid state.

those with two imidazoles, two oxygens and one copper in the higher shells, which is in accordance with X-ray crystallography, but the minima are very shallow.

The results of the best fits for both complexes are shown in Table 7. Figures 7 and 8 compare the k^3-weighted fine structures and Fourier transforms of filtered data and the fits, respectively.

The best fit results always in $R_N < R_O$, independent from starting values of R_N and R_O. This is not in accordance with the data from X-ray crystallography. Due to the already stated fact that the EXAFS commonly cannot discriminate between adjacent elements in the periodic table, there are high correlations between the oxygen and nitrogen parameters. Therfore it is more reliable to look at the average distance values of these two subshells,[17] which are in good agreement with the crystallographic data. In a prior approach with distances fixed at crystallographic values, reasonable values for the Debye−Waller factors were obtained. Whenever attempting to refine all necessary parameters for an unknown system (i.e. distances and Debye−Waller factors), the Cu−N distances of the imidazole were found significantly too short and low or negative Debye−

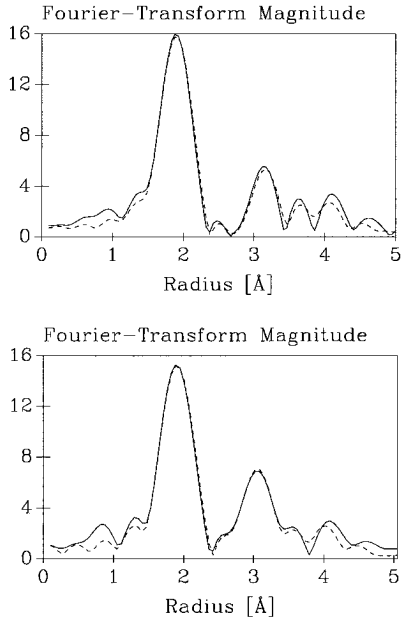

Figure 8. Comparison of the Fourier transforms of the filtered data (solid lines) and the fits (dashed lines) of **3** (top) and **4** (bottom) in the solid state.

Waller factors were obtained for the coordination sphere. The reason for these problems are the high correlations of the parameters within the two subshells.

One of the most important parameters to be derived from this EXAFS study is the Cu−Cu distance. The significance and the value of this interaction is not influenced by the above mentioned correlations. Independent of the fitting procedure used, the parameters obtained for this shell are in close agreement with X-ray crystallography.

According to the present level of knowledge complexes **3** and **4** represent optimal model compounds for catechol oxidase. They imitate the short metal−metal distance as well as the coordination by N/O donor ligands, especially the coordination by two imidazoles and two μ-hydroxo bridges, which has been proposed for the enzyme also.[10] This similarity between the models and the enzyme is further proved by a comparison of the EXAFS spectra and the obtained data from their analysis.[10c,d]

II. Investigations in Methanolic Solution. Before studying the reaction of complexes **3** and **4** with 3,5-di-*tert*-butylcatechol, it is of utmost importance to know their structure in solution, which may be different from that in the crystalline state, because an equilibrium of different complexes with varying stoichiometries is conceivable, e.g., a structure with coordinating solvent molecules instead of the second ligand. In order to check this problem we performed UV−vis titrations and XAS spectroscopic investigations in solution.

UV−Vis Spectroscopy. Solutions of 4×10^{-4} M of the ligands **1** and **2** in methanol were titrated with a solution of copper perchlorate in the same solvent (Figure 9).

The absorptions below 300 nm which belong to aromatic $\pi \rightarrow \pi^*$ transitions are not detectable, because of the surplus of the buffer, which is also aromatic. Both complexes show one absorption maximum between 300 and 320 nm and one between 340 and 370 nm, which can be attributed to π(benzimidazole) → Cu(II) LMCT transitions.[27,28] The d−d bands lie at 620 nm (**3**) and 695 nm (**4**).

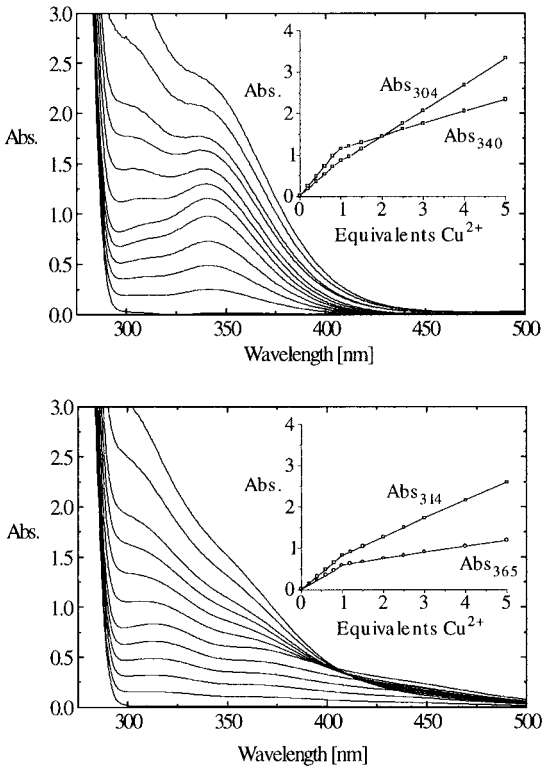

Figure 9. Titration of Hbbp (4×10^{-4} M) (top) and Hbbpen (4×10^{-4} M) (bottom) with $Cu(ClO_4)_2 \cdot 6H_2O$ (0.0, 0.2, 0.4, 0.6, 0.8, 1.0, 1.5, 2.0, 2.5, 3.0, 4.0, and 5.0 equiv). The inserts show plots of two absorption maxima against the copper concentration.

The plots of the absorption maxima between 300 and 370 nm against the added amounts of Cu^{2+} ions to the ligands show a linear correlation up to a stoichiometry of 1:1 (Cu^{2+}/ligand). At this point there is a sharp bend, after which the line runs linear again. This result suggests that, as long as there is enough of the ligand, only one complex species with the same stoichiometry as in the crystalline state is formed. After all of the ligand is used up, another species (the solvent or the buffer) coordinates to the excess copper ions. A further proof for the uniformity of the reactions is the presence of an isobestic point (Figure 9, bottom).

X-ray Absorption Spectroscopy. In order to prove the obvious supposition that the complex species, which are formed in solution and which have the same stoichiometries as in crystalline state, also have the same structures, we performed XAS measurements in solution and compared them with the measurements in the solid state.

The similarity of the edge spectra of the complexes in the two different states is shown in Figure 5.

The comparison between the k^3-weighted fine structures of the unfiltered data and the Fourier transforms is shown in Figures 10 and 11, respectively.

For comparison of the plots, it is important to keep in mind the different conditions while the spectra are recorded. The spectra of the models in the solid state were recorded in absorption mode at 20 K at the HASYLAB, Hamburg, whereas the compounds in solution were measured in fluorescence mode at room temperature (**3**) or at 80 K (**4**) at the SRS, Daresbury. The concentration of the solution samples is lower than the concentration of the solid state samples, which results in a higher noise level for the solution spectra. Despite the different detection techniques and temperatures, the spectra and Fourier transforms of the k^3-weighted fine structures of **4** in both states

(27) Casella, L.; Carugo, O. *Inorg. Chem.* **1993**, *32*, 2056.
(28) Dagdigian, J. V.; McKee, V.; Reed, C. A. *Inorg. Chem.* **1982**, *21*, 1332.

Table 8. Results of the First-Shell Fits[a] and the Second-Shell Fits[a] (Metal−Metal Contribution) by Curve-Fitting Analysis of the Complexes in Solution

complex	window width,[b] Å	N_{free}[c]	cn[d] and scatterer	R, Å	σ^2, Å^2	E_0	R-factor,[c] %
			First Shell				
3 in solution	1.0−2.0	6	4.5 O	1.898	0.010	14.4	12.4
			or 5.2 N	1.921	0.009	15.4	15.5
4 in solution	1.0−2.1	8	2.8 O	1.948	0.002	10.1	16.5
			or 3.3 N	1.966	0.002	11.6	15.9
4 in solution	1.0−2.0	6	1.3 O	1.849	0.003	16.8	10.4
after addition of 3,5-DTBC			or 1.7 N	1.869	0.003	18.2	11.4
			Second Shell				
3 in solution	2.4−3.2	5	0.7 Cu	3.031	0.005	9.5	10.9
4 in solution	2.4−3.2	6	0.6 Cu	2.977	0.001	13.2	14.0
4 in solution	2.0−2.9	6	0.7 Cu	2.783	0.008	24.3	16.9
after addition of 3,5-DTBC							

[a] The Fourier transform range is about $k = 1.6-12.5$ Å^{-1}. [b] The window width for Fourier filtering is given in reduced angstroms. [c] As defined in the Experimental Section. The number of refined parameters is 4 for all fits and therefore less than the maximum number of free parameters. [d] cn = coordination number.

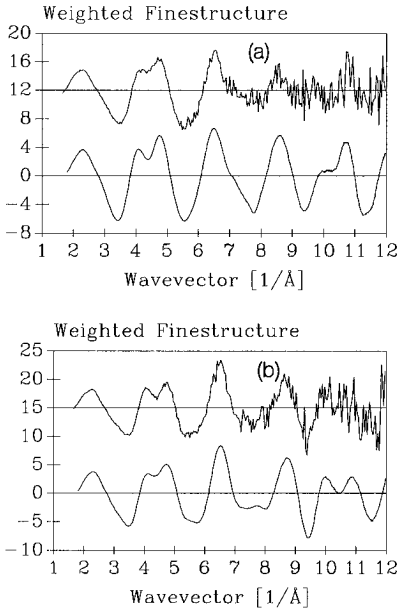

Figure 10. Comparison of the k^3-weighted fine structures of the unfiltered data in the solid state (bottom) and in solution (top) of **3** (a) and **4** (b).

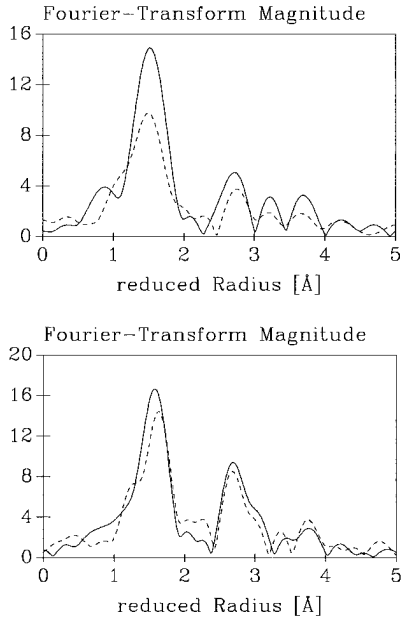

Figure 11. Comparison of the Fourier transforms of the k^3-weighted fine structures in the solid state (solid lines) and in solution (dashed lines) of **3** (top) and **4** (bottom).

are extremely similar. One has to be cautious to compare data of differently concentrated samples received from different measurement techniques,[29] but it is obvious that this is not a problem here. Comparing the plots for **3**, the higher thermal disorder of the solution data is clear. This results particularly in a weakening of the higher shell contributions, which can be seen in the high-k range of the k^3-weighted fine structure. Furthermore the peaks in the Fourier transform of the k^3-weighted fine structure indeed appear at the same distances as the peaks of the solid state data, but they are broadend due to higher Debye−Waller factors.

The results of the curve-fitting analysis of the first shell and the second shell (metal−metal contribution) of the Fourier-filtered EXAFS data are shown in Table 8.

Within the estimated error range, which is somewhat higher for the solution data than for the solid state data because of the higher noise level, the obtained structural parameters are nearly the same. The Debye−Waller factors for **3** in solution are significantly higher than in solid state, as was expected because of the high temperature difference of these two measurements. The results of the wide-shell fits including multiple scattering contributions, which were performed in the described way, are also similar with those of the solid state data. The corresponding tables and plots can be requested from the authors.

By independent experimental techniques it was proven that in a 2,4,6-collidine/$HClO_4$ buffered methanolic solution of copper perchlorate and the ligands used in this work (ratio 1:1) only one complex species is formed, namely, the one which also crystallizes and is described here.

III. Reaction with 3,5-Di-*tert*-butylcatechol (3,5-DTBC). UV−Vis Spectroscopy. The detection of the oxidation of 3,5-di-*tert*-butylcatechol (3,5-DTBC) to the corresponding *o*-quinone (3,5-DTBQ) can be followed by the development of the absorption band at about 400 nm ($\epsilon = 1900$ M^{-1} cm^{-1}) in methanol.[30] No such band appears after addition of 3,5-DTBC to a solution of **3**, which means that this complex shows no activity toward the oxidation of catechols. The course of the same reaction with a solution of **4** is shown in Figure 12.

(29) Bertagnolli, H.; Kaim. W. *Angew. Chem.* **1995**, *107*, 847. Bertagnolli, H.; Kaim. W. *Angew. Chem., Int. Ed. Engl.* **1995**, *34*, 770.

(30) Flaig, W.; Ploetz, Th.; Kullmer, A. *Z. Naturforsch., B* **1955**, *10*, 668.

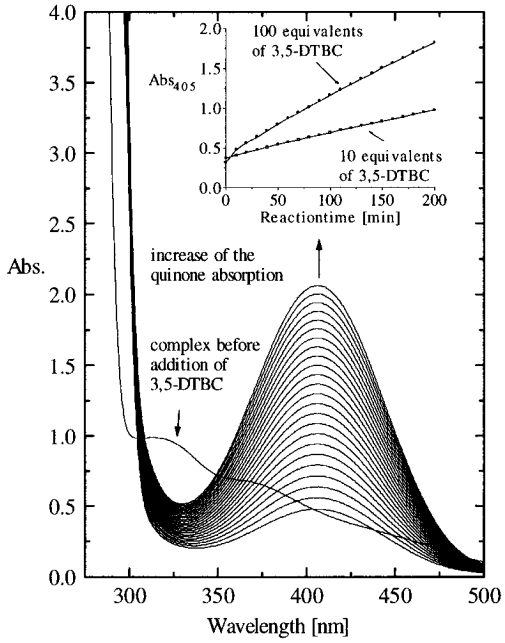

Figure 12. Increase of the quinone band after addition of 3,5-di-*tert*-butylcatechol (3,5-DTBC) (100 equiv) to a solution of **4** (4×10^{-4} M) in methanol. The spectra are recorded every 10 min. The insert shows the course of the absorption maximum at 405 nm with the time for 10 and 100 equiv of 3,5-DTBC.

A few seconds after addition of 3,5-DTBC to a solution of **4**, the π(benzimidazole) → Cu(II) LMCT transitions between 320 and 400 nm vanish, which can be explained either by the complete destruction of the complex (which is improbable, because the chelating ligand Hbbpen is a stronger ligand than the solvent, catechol or quinone), or by the formation of Cu(I), which is more probable. Simultaneously the quinone absorption at 405 nm appears. Its extinction reveals a turnover of 1 equiv. After this fast stoichiometric first step the quinone absorption increases linearly, depending on the catechol concentration.

X-ray Absorption Spectroscopy. Due to the inactivity of complex **3** in solution concerning the catechol oxidation, we did not perform XAS measurements of this sample in the presence of catechol.

The interpretation of the UV−vis spectrum of complex **4** in solution after addition of 3,5-DTBC suggests the reduction of Cu(II) to Cu(I). The XANES region allows one to differentiate unambiguously between these two oxidation states. The XANES spectrum is shown in Figure 5. The edge is shifted by about 9 eV to lower energy compared to the solution of **4** without 3,5-DTBC, which reveals a reduction of the oxidation state of the absorber atom.[31] There is no pre-edge peak at about 8979 eV, which is assigned to a 1s → 3d transition in Cu(II) und which is not existing in a Cu(I) edge spectrum. Furthermore, a strong peak appears at 8983 eV (normalized intensity: 0.93), which is assigned to a 1s → 4p transition in Cu(I) and does not appear in XANES spectra of Cu(II).[24a,32] Kau et al.[24a] have shown for a range of two-, three-, and four-coordinated Cu(I) complexes that the position and intensity of this peak is dependent on the site geometry of the central atom. The latter complexes exhibit a peak position higher than 8985.5 eV with an intensity lower than 0.8 and therefore a four-coordination can be excluded in our case. Compared to the four-coordinated Cu(I) complexes the peaks of the other complexes are shifted 1.5−2.5 eV to lower energy and have intensity values of 1.08 ± 0.10 (two-coordination) and of 0.63 ± 0.05 (three-coordination). Thus the interpretation of the XANES region suggests that after addition of 3,5-DTBC the present complex is reduced to two- or three-coordinated Cu(I).

Scheme 1

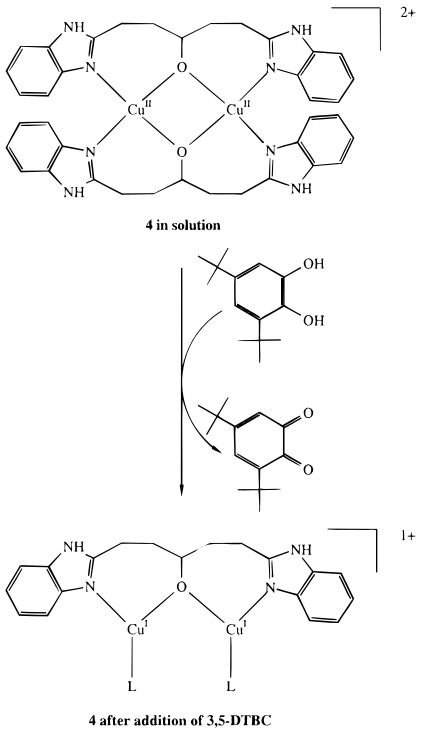

The results of the curve-fitting analysis of the first shell and the second shell (metal−metal contribution) of the Fourier-filtered EXAFS spectra of this sample, recorded at room temperature, are shown in Table 8. Concerning the first shell data, a comparison to the complex without 3,5-DTBC reveals a significant decrease of the coordination number and the absorber−scatterer distances. Due to the estimated error range of ±1 for the coordination number, it is not possible to distinguish between two- and three-coordination from EXAFS. A linear two-coordinated dinuclear Cu(I) complex bridged by the alkoxo oxygen atom of the ligand can be ruled out for sterical reasons. Therefore, in the case of a two-coordination, we have to assume a mononuclear complex. In it the metal can be coordinated by the ligand **2**, the solvent, the substrate, the product, or even the buffer, whose sterical repulsions due to the methyl groups would only be small for a linear, staggered coordination. In all of these cases the relatively strong second shell peak in the Fourier transform of the k^3-weighted fine structure at about 2.8 Å would be caused by the carbon atoms of the coordinating ligands. Such a fit of the filtered peak did not yield satisfactory results (high *R*-factor, very low Debye−Waller factor and coordination number), whereas the fit of this peak as a copper scatterer yields good results, which are similar to those of the other metal−metal scattering contributions (Table 8). Therefore, we suggest a dinuclear, bridged Cu(I) complex, where the copper atoms are three-coordinated. Two coordination sites are used by the ligand **2** (one alkoxo oxygen and one benzimidazole nitrogen); the third coordination site could be used by the solvent, the buffer, the product, or a second ligand molecule with a uncoordinating alcohol(ate) group (named as L in Scheme 1, which is formulated for the first, fast, and stoichiometric step of the reaction of 3,5-DTBC with **4** in solution). It is not possible to differentiate between these possibilities by EXAFS or UV−vis.

(31) Agarval, B. K.; Verma, L. P. *J. Phys. C* **1970**, *3*, 535.
(32) Blackburn, N. J.; Strange, R. W.; Reedijk, J.; Volbeda, A.; Farooq, A.; Karlin, K. D.; Zubieta, J. *Inorg. Chem.* **1989**, *28*, 1349.

Table 9. Results of the Wide-Shell Fit[a] Using Multiple Scattering Calculations and Constrained Refinement of the Imidazole Groups for Complex **4** in Solution after Addition of 3,5-DTBC

complex	window width,[b] Å	N_{free}[c]	cn[d] and scatterer	R, Å	σ^2, Å^2	E_0	ϕ, deg	R-factor,[c] %
4 in solution	1.0−4.5	23	2 O	*1.929*	*0.033*	*15.8*	*127.2*	20.6
after addition of 3,5-DTBC			1 N (imi)	*1.873*	*0.001*			
			1 C (imi)	2.902	*0.011*[e]			
			1 C (imi)	2.917	0.011[e]			
			1 N (imi)	4.039	*0.010*[f]			
			1 C (imi)	4.132	0.010[f]			
			1 Cu	*2.807*	*0.012*			

[a] The Fourier transform range is $k = 1.6-12.3$ Å^{-1}. [b] The window width for Fourier filtering is given in reduced angstroms. [c] As defined in the Experimental Section. The number of refined parameters is 10 and therefore less than the maximum number of free parameters. [d] cn = coordination number, not refined. [e] Refined together. [f] Refined together, see Experimental Section. All refined parameters in italics.

The results of the multiple scattering fit of the wide-shell filtered data initiated by the proposed structure of **4** in solution after addition of 3,5-DTBC are given in Table 9.

Again the parameters for the coordinating oxygen and nitrogen atoms are highly correlated, which leads to similar problems during the fitting procedure as described for the models in solid state. Despite this, the results of the multiple scattering fit are in accordance with the results of the single-shell fits. Due to the lower coordination number, the absorber−scatterer distances and therefore the metal−metal distance also are significantly lower for the complex after addition of 3,5-DTBC. A comparison of the k^3-weighted fine structures and the Fourier transforms of the filtered data and the fits is shown in Figure 13.

The further increase of the quinone band in the UV−vis spectrum after the stoichiometric first step can be explained by a slow oxidation of the Cu(I) complex to Cu(II) by air oxygen. The Cu(II) complex is reduced immediately to the Cu(I) complex again, as long as 3,5-DTBC is present.

Finally, it has to be explained why the copper complex with ligand **2** is able to oxidize catechol, whereas a solution of the similar complex with ligand **1**, which differs only by two CH_2 groups, cannot do so. The six-membered chelate rings formed by the ligand in **3** have a stable twisted conformation, whereas the seven-membered chelate ring in **4** should be less stable. The flexibility of ligand **2** in complex **4** becomes apparent in the disordered coordinating methanol in the crystal structure together with the large thermal ellipsoids, especially of the chelate ring carbon atoms. This ligand flexibility is an essential condition for the reactivity of the complex.

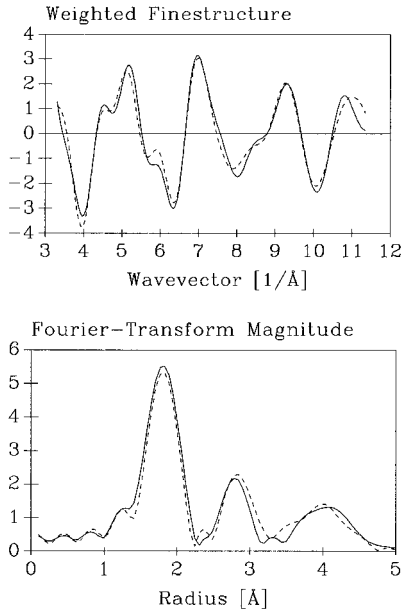

Figure 13. Comparison of the k^3-weighted fine structures (top) and the Fourier transforms (bottom) of the filtered data (solid lines) and the fits (dashed lines) of **4** after addition of 3,5-DTBC.

Acknowledgment. We especially thank Dr. Fred Mosselmans from the Synchrotron Radiation Source, SERC Daresbury Laboratory for his technical assistance at the beam line recording the XAS spectra and for the useful discussions. Financial support from the Bundesminister für Forschung und Technologie, from the Deutsche Forschungsgemeinschaft, from the Fonds der Chemischen Industrie, and from the European Community is gratefully acknowledged.

Supporting Information Available: Figures showing unit cells and magnetic data plots and tables listing crystallographic parameters, including atomic coordinates, anisotropic thermal parameters, and complete bond distances and angles of complexes **3** and **4** (11 pages). Ordering information is given on any current masthead page.

IC9513604